

Unary Adsorption of Phthalates from Wastewater onto Water Hyacinth Biochar: Parameters, Drivers and Mechanism

Elkanah N. Ogora¹ , Zachary M. Getenga² , Joel M. Gichumbi¹, Victor O. Shikuku^{3*} 

¹Department of Physical Sciences, Chuka University, Kenya.

²Department of Physical Sciences, Machakos University, Machakos, Kenya.

³Department of Physical Sciences, Kaimosi Friends University, Kaimosi, Kenya.

ABSTRACT

In this study, water hyacinth root-derived biochar (WHB) was prepared as a low-cost adsorbent for the removal of three phthalates, namely, benzyl butyl phthalate (BBP), dimethyl phthalate (DMP) and bis(2-ethylhexyl) phthalate (BEHP) from single solute aqueous solutions. The equilibrium data were best described by the adsorption isotherm models in the order Freundlich>Langmuir>Dubinin-Radushkevich-Kaganer (D-R-K) isotherms. The maximum monolayer adsorption capacity (Q_o) was 1.83, 1.77, and 1.62 mg/g for DMP, BBP, and BEHP, respectively. The adsorption of the phthalates was diminished by increased molecular weight and molar volume of the molecules but compensated by their hydrophobicity. The kinetic data were best described by the pseudo-second order (PSO) model and pore diffusion was not the sole operative rate-determining step. The calculated thermodynamic functions, changes in Gibbs free energy ($\Delta G < 0$), enthalpy ($\Delta H < 0$), and entropy ($\Delta S < 0$) demonstrate the adsorption of DMP, BBP, and BEHP onto WHB is energetically favorable, exothermic, spontaneous and of a physical type controlled by hydrophobic interactions. The comparative adsorption capacities imply that WHB would sequester phthalates regardless of their physicochemical profiles.

KEYWORDS

Phthalates, Water hyacinth biochar, adsorption, physicochemical properties

Received 1 October 2024, revised 11 November 2024, accepted 13 March 2025

INTRODUCTION

Endocrine-disrupting chemicals (EDCs) are chemical substances that disturb the functionality of the endocrine system in both animals and humans. They interfere with natural hormone cycles, specifically affecting reproduction, development, metabolism, and growth.¹ Most endocrine-disrupting chemicals are man-made.² Unfortunately, these EDCs have been reported in groundwater, oceans, lakes, marine, and food products, posing a potential risk to both aquatic and terrestrial life forms.^{3,4} They have negative health effects on male and female reproductive systems (natural estrogen and androgens), thyroid and breast development, and cause birth defects and obesity.⁵ Examples of EDCs reported in water resources include persistent organic pollutants (POPs), pesticides, pharmaceuticals and personal care products (PPCPs), and per- and polyfluoroalkyl substances (PFAS).⁶ Complete removal of these contaminants from drinking water is therefore critical. Among the POPs with endocrine disruption potential reported in effluents from wastewater treatment plants (WWTPs) are phthalates.⁴ This indicates that WWTPs are point sources of phthalates loading into recipient water bodies, a testament that these traditional WWTPs are not designed to sequester phthalates from water. Alternative approaches are required. Phthalates are potentially carcinogenic, have been linked to infertility and even birth defects are some of the harmful effects.⁷ Approaches for the removal of water contaminants include adsorption, membrane filtration, ion exchange treatment, advanced oxidation process (AOPs), precipitation, and solvent extraction.⁸ Unfortunately, some of these techniques, such as AOPs, require intensive capital investment thus making them unsustainable, especially in rural areas in low-income countries.⁹ Some of the materials reported as possible adsorbents for the removal of phthalates include activated carbons,¹⁰ polymer resins,¹¹ carbon nanotubes,¹² chitosan¹³ and seaweed biosorbent¹⁴ among others. Adsorption onto biomass

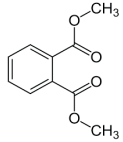
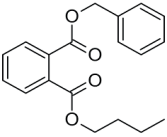
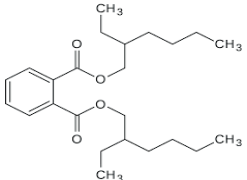
waste-derived adsorbents has been demonstrated as an alternative and sustainable method for the removal of organic micropollutants from water due to its eco-friendliness, efficiency, cost-effectiveness, simplicity, and availability of these feedstocks even in remote places.¹⁵ The aforementioned studies show that the adsorption characteristics of biomass-based adsorbents depend on the type of feedstock and the adsorbent preparation conditions. Furthermore, the adsorption kinetics and adsorption capacity are also a function of the molecular properties such as molecular weight, kinetic diameter, solubility, and functional group density of the phthalates.¹⁶ For a given adsorbent, it is important to evaluate the interplay of these factors to optimize the performance.

Water hyacinth (WH), an aquatic weed prevalent on the Kenyan side of the Lake Victoria basin, presents a suitable candidate for biomass-based adsorbent development with concomitant environmental benefits. While water hyacinth-derived biochar (WHB) has been reported as a suitable material for the removal of antibiotics from water,¹⁷ heavy metals,¹⁸ pesticides,¹⁹ and industrial chemicals,²⁰ to date, there has been no study of the adsorption characteristics (rates and capacity) of WHB for the removal of phthalates as influenced by both environmental conditions and the physicochemical properties of the phthalates. For WHB to be considered a next-generation adsorber, its ability to adsorb a broad spectrum of pollutants and the associated drivers must be evaluated.

The objective of this study was to symmetrically evaluate the adsorption of three phthalates, namely, dimethyl phthalate (DMP), benzyl butyl phthalate (BBP), and Bis(2-ethylhexyl) phthalate (BEHP), onto WHB. The compounds were selected as probe molecules for their recalcitrance to conventional WWTPs techniques and occurrence in treated effluents²¹ and for their varied chemical structures and molecular properties as shown in Table 1²² that influence their environmental partitioning.

*To whom correspondence should be addressed
Email: vshikuku@kafu.ac.ke

Table 1: Physicochemical properties of phthalates (log K_{ow} is the octanol-water partition coefficient, a measure of a compound's hydrophobicity, LeBas molar volume is the molar volume of a molecule).

Name	Structure	Molecular weight	Solubility in water (mg/L)	log K_{ow}	LeBas molar volume (cm ³ /mol)
DMP		194.2	4200	1.5-2.1	206.4
BB BPB		312.4	2.7	4.8	364.8
BEHP		390.57	0.003	8.8	520.4

Source: Cousins et al. (2003)²²

MATERIALS AND METHODS

Chemicals, reagents and apparatus

The standards (99.9% purity) of DMP, BBP, and BEHP, analytical grade methanol, de-ionized water, glass wool filter papers, and 0.45 µm glass micro filters were purchased from Kobian Scientific Ltd, Kenya.

Adsorbent preparation

The water hyacinth (*Eichhornia crassipes*) was collected from Lake Victoria, in Kisumu City (0°5'30.1" S, 34°46'4.8" E), Kenya. The roots were cut into pieces and washed with distilled water to remove all the dirt and air dried. Biochar preparation was done through a slow-pyrolysis temperature of 350 °C, at a heating rate of 10 °C/minute for 1 hour using a furnace. The sample was then washed using distilled water. It was oven-dried at the temperature of 100°C for a period of 2 hours.²³ The resulting sample (WHB) was sieved through a 212 µm sieve and stored for adsorption experiments.

Adsorbent characterization

Elemental analysis of WHB was carried out using an XRF (Brucker, S1 TITAN, Germany). The surface functional groups in the WHB were inspected using FTIR (IRAffinity-1S, Shimadzu) between 4000 and 400 cm⁻¹ wavenumbers. Crystallinity and mineral phases were determined by XRD.

Effect of contact time

A mass of 0.1 g of WHB was placed in a 250 mL conical flask containing 50 mL of a 10 mg/L phthalate solution and agitated at 125 rpm using an orbital shaker at room temperature. At regular time intervals of 5 minutes (5, 10, 15, 20, 25, 30, 35, 40, and 50 min), the residual concentrations of phthalate in the solution were determined by HPLC (Thermos Scientific Dionex UltiMateTM 3000 HPLC system). The mobile phase consisted of methanol and water in a 80:20 v/v ratio, operating in isocratic mode. A, a C18 reverse phase HPLC column maintained at 35 °C and, a mobile phase flow rate of 10 µL/min was used, and column temperature maintained at 35 °C. The amounts of phthalate (mg/g) adsorbed onto WHB per unit mass (q_e) at any given time (t) were determined as:

$$q_e = \frac{(C_0 - C_e)V}{m} \quad (1)$$

where C_0 and C_e are the initial and equilibrium phthalate concentrations (mg/L), respectively. m is the mass (g) of the WHB used, and V is the volume of the solution (L). The experimental data obtained were fitted to three kinetic models:

Pseudo-first-order (PFO):²⁴

$$\log(q_e - q_t) = \log q_e - \frac{k_1}{2.303}t \quad (2)$$

Pseudo-second-order (PSO):²⁵

$$\frac{t}{q_t} = \frac{1}{k_2 q_e^2} + \frac{1}{q_e}t \quad (3)$$

Intra-particle diffusion (IPD) model:²⁶

$$q_t = k_p t^{0.5} + C \quad (4)$$

where t (minutes) and q_t (mg/g) are the time and amount adsorbed at equilibrium time, respectively, while q_e is the equilibrium adsorption capacity. Also, k_1 , k_2 , and k_p are rate constants for PFO, PSO, and IPD models, respectively. The intercept C is related to the mass transfer across the boundary.

Effect of initial concentration

Masses of 0.1 g of WHB were separately, put into 50 ml of phthalate solutions with varying concentrations ranging between 4 to 12 mg/L (4, 6, 8, 10, and 12 mg/L) done at 298 K and then agitated at 125 rpm for 25 min. The residual phthalate in the solution was then determined.

The experimental data were then fitted to linearized Langmuir, Freundlich isotherm and Dubinin-Radushkevich-Kaganer (D-R-K) isotherm models,²⁷⁻³⁰ shown in Table 2. In Table 2, q_e (mg/g) and C_e (mg/L) are the solute concentration on the adsorbent and in the bulk solution at equilibrium, respectively. Q_0 (mg/g) is the maximum monolayer adsorption capacity, while q_s and ϵ are theoretical isotherm saturation capacity (mg/g) and Polanyi potential, respectively. R_L is the dimensionless Langmuir separation constant. The K_L (L/g), K_f and K_{ads} (mol²/kJ²) are Langmuir, Freundlich, and D-R-K isotherm constants, respectively. The exponential factor $\frac{1}{n}$ is related to the adsorption affinity and surface heterogeneity.³¹ The constants R and T represent the universal gas constant (8.314 J/K.mol) and temperature (K), respectively.

Effect of temperature

The effect of temperature change on the adsorption of selected phthalates onto WHB was studied in the range of 298–338 K. A mass of 0.1 g of WHB was put into 50 mL of 10 mg/L solutions of each phthalate compound and the solutions in triplicates agitated at different temperatures (298, 308, 318, 328 and 338 K) until equilibration. The thermodynamic parameters, ΔG , ΔH and ΔS , were estimated using the equations below:

$$\Delta G = RT \ln K_c \quad (5)$$

$$K_d = \frac{C_{ad}}{C_e} \quad (6)$$

$$K_c = 1000 K_d \quad (7)$$

$$\ln K_c = \frac{\Delta S}{R} - \frac{\Delta H}{RT} \quad (8)$$

where K_c is the equilibrium constant (dimensionless), C_e is the equilibrium concentration in the solution (mg/L) and C_{ads} is the equilibrium solid phase concentration (mg/g). K_d is the distribution coefficient (L/g), R is the gas constant ($8.314 \text{ J mol}^{-1} \text{ K}^{-1}$) and T is the temperature in Kelvin.

The data was further modeled using three classical adsorption isotherms, namely Langmuir, Freundlich and Dubinin-Radushkevich-Kaganer (D-R-K) isotherms. From the D-R-K isotherm, the mean adsorption energy E_a (kJ/mol), that provides insight on physisorption, and chemisorption mechanisms was calculated using:

$$E_a = \frac{1}{\sqrt{2} k_D} \quad (9)$$

Effect of adsorbent dosage

To 50 mL of 10 mg/L of the phthalate solutions, different weighed amounts of adsorbent (0.2, 0.4, 0.6, 0.8, 1.0, and 1.2 g) were dispersed at 298 K and agitated at 125 rpm until equilibration. All the other parameters were kept constant. The percentage of phthalate removed was calculated using:

$$\%R = \frac{C_0 - C_e}{C_0} \times 100 \quad (10)$$

RESULTS AND DISCUSSION

Elemental composition of WHB

The elemental percent composition of the WHB obtained by XRF analysis is presented in Table 3. The absence of toxic heavy metals indicates that the biochar is unlikely to cause secondary pollution during application through the leaching of toxic heavy metals into the aqueous solution.

Functional group analysis

The functional groups present and the variation in their vibrational frequencies after adsorption were inspected using FTIR spectroscopy. The IR spectra as shown are shown in the Figures 1 and 2.

The band 3464.28 cm^{-1} , before adsorption, and 3506.15 cm^{-1} , after adsorption represented the stretching vibrations of the -OH group. This group was due to the water adsorbed on the biochar.³² The band centered at 2925.76 cm^{-1} observed after adsorption was assigned to C-H stretching aliphatic functional groups from the phthalates and provides evidence for adsorption.³³ The bands between 1636.92 cm^{-1} and 1635.65 cm^{-1} for WHB before adsorption and after adsorption

Table 2: Isotherm equations and parameters

Isotherm Model	Equation	Parameters	Reference
Langmuir	$\frac{1}{q_e} = \frac{1}{Q_o} + \frac{1}{Q_o K_L C_e}$	Q_o (mg/g), K_L (L/g)	27
	$R_L = \frac{1}{1 + K_L C_o}$	R_L	28
Freundlich D – R model	$\log q_e = \log K_f + \frac{1}{n} \log C_e$	K_f , n	29
	$\ln q_e = \ln q_s - k_{ads} \varepsilon^2$	K_{ads} (mol^2/kJ^2)	30
	$\varepsilon = RT \ln \left\{ 1 + \frac{1}{C_e} \right\}$	q_s (mg/g)	

Table 3: Elemental composition of WHB before and after adsorption

Element	Percentage of Element Present in WHB			
	Before Adsorption	+/- [*3]	After Adsorption	+/- [*3]
Al	10.600	0.727	11.125	0.775
Si	24.025	0.644	25.561	0.697
P	0.347	0.074	0.233	0.074
S	1.547	0.051	0.411	0.040
Cl	2.014	0.025	0.249	0.020
K	5.332	0.055	4.758	0.054
Ca	2.442	0.040	1.734	0.036
Ti	0.997	0.016	1.011	0.017
Cr	0.007	0.005	0.000	0.006
Mn	1.101	0.028	1.774	0.031
Fe	11.870	0.074	12.250	0.077

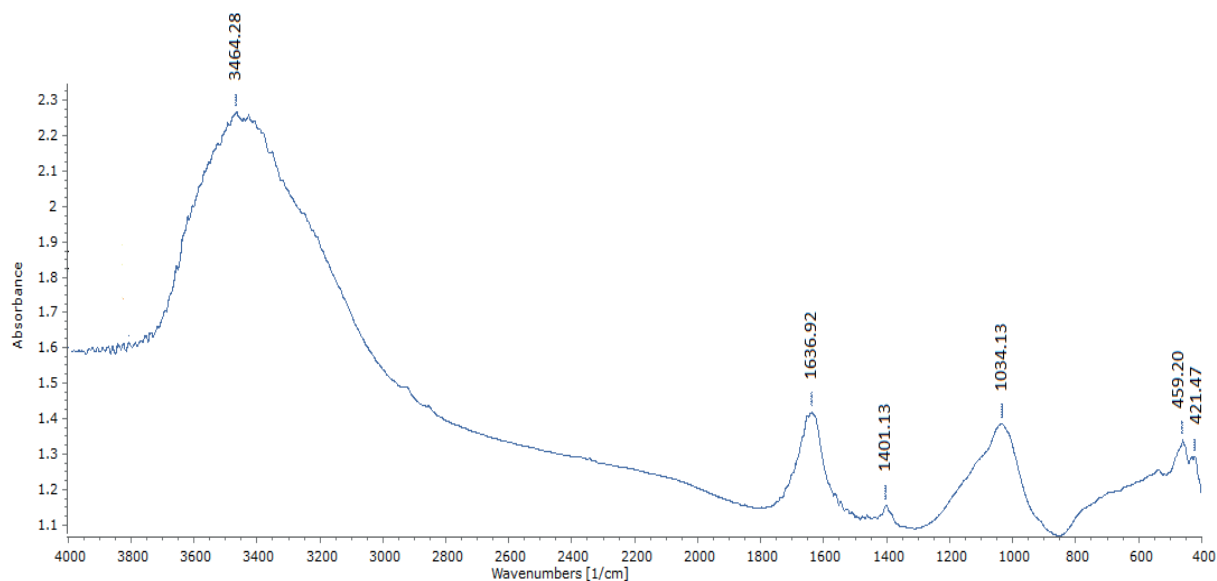


Figure 1: FTIR spectrum of WHB before adsorption

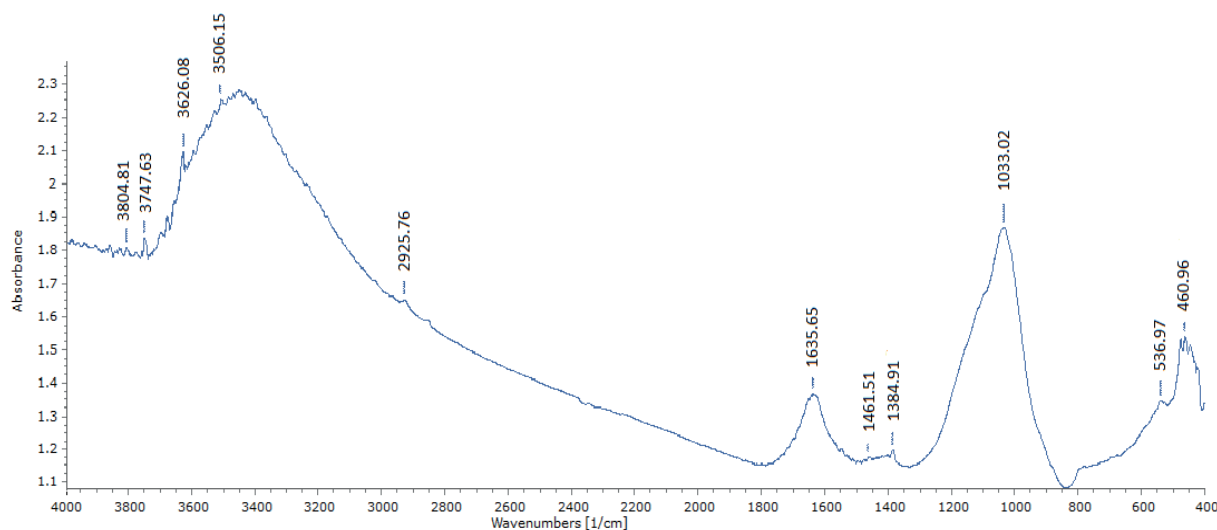


Figure 2: FTIR spectrum of WHB after the adsorption process

respectively, were found to be stretching vibration of OH deformation of water, and aromatic C=O stretching vibration of the carbonyl from the carboxyl group, respectively.³³

The bands at 1401.13 cm^{-1} and 1461.51 cm^{-1} represent the COO⁻ groups and C-H deformation vibrations, respectively. The band at 1384.91 cm^{-1} is attributed to C-H in-plane bending vibrations. The broad bands at 1034.13 cm^{-1} and 1033.02 cm^{-1} before and after adsorption, respectively, may be attributed to the C-O bending vibration or the band of the out-of-plane bending for carbonates (CO_3^{2-}) or P-O bond of phosphate in the biochar. The minor shifts in the absorption bands indicate changes in the chemical environments of these functional groups and demonstrate weak interactions between the phthalates and the biochar functional groups. This provides circumstantial evidence for a physisorption mechanism.

Effect of contact time

The effect of contact time is essential in determination of the residence time of a water treatment process. In this work, equilibration was attained in 25 minutes beyond which there was no appreciable change in the amount adsorbed (mg/g) (Figure 3). The percent removal (%R) at equilibrium were 76.59%, 75.98% and 75.49% for DMP, BBP and BEHP, respectively.

The data was further fitted to the quasi-first order (PFO), quasi-second order (PSO) and intra-particle diffusion (IPD) kinetic models to gain insight on adsorption rates and mechanisms involved. The kinetic parameters are summarized in Table 4.

From Table 4, the low coefficient of determination (R^2) values and the wide variance between the experimental equilibrium adsorption capacity ($q_{e(\text{exp})}$) and the model-predicted values ($q_{e(\text{cal})}$) reveal that the PFO poorly fits the experimental data. The adsorption of phthalates onto WHB is therefore not a PFO reaction. On the other hand, the close agreement between the PSO-predicted values and the experimental values with R^2 values closest to unity (Table 4) shows that the PSO kinetic model best described the adsorption data. The PSO model infers a chemisorption-mediated adsorption process in the rate-determining step. The adsorption rates, denoted by k_2 , were independent of the molecular weight of the phthalates. This implies an intricate interplay between hydrophobicity, kinetic diameters, functional groups, and accessibility to active binding sites.

Figure 4 depicts the IPD model plot for DMP. The multi-linear plots show that several mechanisms are involved in the adsorption process with significant boundary layer effects.¹⁷ The C values are an index of the mass transfer across the boundary layer. The greater the magnitude of C, the greater the boundary layer effect.¹⁷ From Table 4,

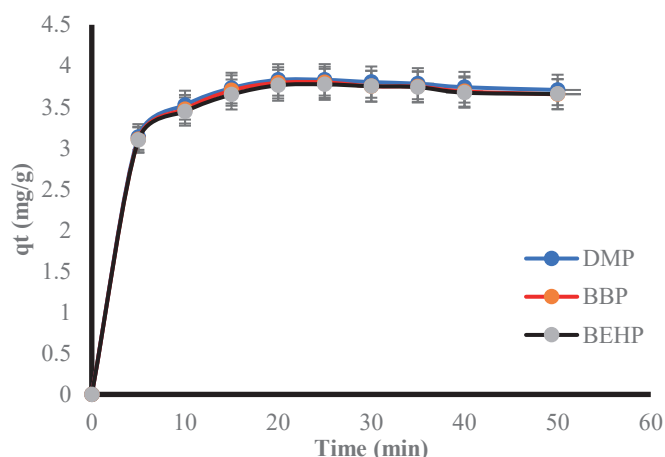


Figure 3: Variation of amount adsorbed with time

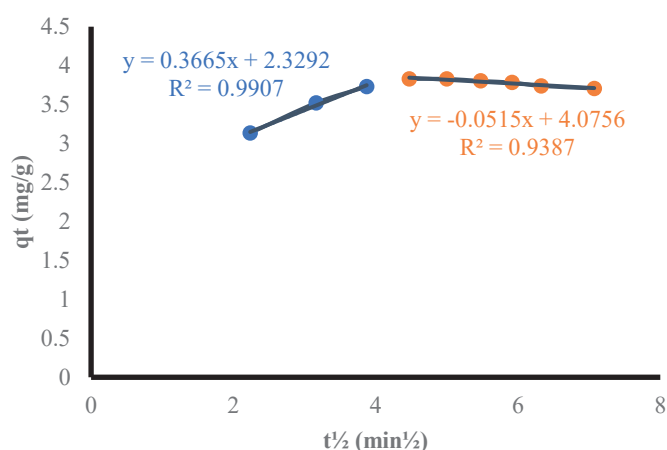


Figure 4: IPD diffusion model of DMP adsorption onto WHB

Table 4: PFO and PSO kinetic parameters

Adsorbate	PFO model			
	$q_{e(\text{exp})}$ (mg/g)	$q_{e(\text{cal})}$ mg/g	K_1	R^2
DMP	3.788	0.7468	-0.0555	0.197
BBP	3.733	0.5446	-0.0233	0.056
BEHP	3.740	0.7104	-0.0269	0.109
	PSO model			
	$q_{e(\text{exp})}$ (mg/g)	$q_{e(\text{cal})}$ mg/g	K_2	R^2
DMP	3.788	3.830	0.725	0.999
BBP	3.733	3.799	0.983	0.998
BEHP	3.740	3.775	0.655	0.999
	IPD model			R^2
	k_p (mg.g ⁻¹ /min)	C		
DMP	0.100	3.191	0.487	
BBP	0.097	3.168	0.459	
BEHP	0.101	3.125	0.519	

the non-zero interception implies that pore diffusion is not the sole operative adsorption mechanism. The interceptions obtained from all the adsorption cases are attributed to a wide range of pore sizes of the WHB.³⁴

Adsorption isotherms

When the initial concentration was increased from 1 to 4 mg/L, the percent removal (%R) increased to a maximum of 37.99%, 35.28%, and 34.81% for DMP, BBP, and BEHP, respectively (Figure 5). This is attributable to the large number of vacant active sites and increased mass gradient between the bulk solution and the solid phase. However, beyond 4 mg/L the percent removal consistently decreased is beyond 4 mg/L. This decrease is due to the saturation of the limited number of active and energetically favorable adsorption sites of the WHBWBH and increased repulsion between the adsorbed phthalate molecules and those in the bulk solution.³⁵

The data was further modeled using three classical adsorption isotherms, namely Langmuir, Freundlich and Dubinin-Radushkevich-Kaganer (D-R-K) isotherms, and their plots are shown in Figures 6, 7 and 8, respectively. The calculated constants are presented in Table 5.

From the Langmuir isotherm, the maximum adsorption capacity (Q_0) decreased in the order DMP>BBP>BEHP (Table 5) with increasing molecular weight and LeBas molar volume (Table 1). This shows that the adsorption capacity was controlled by the molecular weight and kinetic diameters of the phthalates. Furthermore, the adsorption capacities are comparable despite the wide variances in molecular weights and Lebas molar volume. This is due to the

compensation effect of increasing hydrophobicity ($\log K_{ow}$) (Table 1), an indication that hydrophobic interactions were significant as the driving adsorption mechanism. This is further supported by the Freundlich affinity factors K_F that were comparable across the phthalates. The $1/n$ values below unity denote a heterogeneous WHB surface with energetically different binding sites. Additionally, the low $1/n$ values signify weak adsorbate-adsorbent interactions consistent with the physisorption mechanisms from the FTIR study.³⁶ The R_L values ($0 < R_L < 1$) show that the adsorption of the selected phthalates onto WHB was deemed favorable.³⁷

The D-R isotherm did not show good linear regression with the adsorption of the selected phthalates, relative to the other models. Its low mean free energy ($E = 0.01$ kJ/mol) suggests a physisorption adsorption process.³⁸

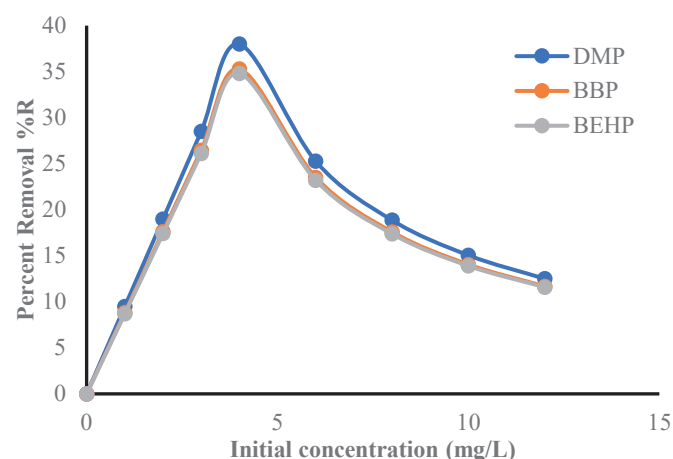
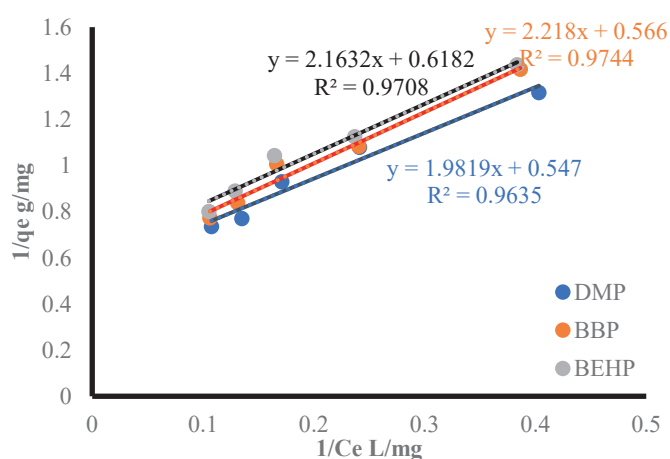
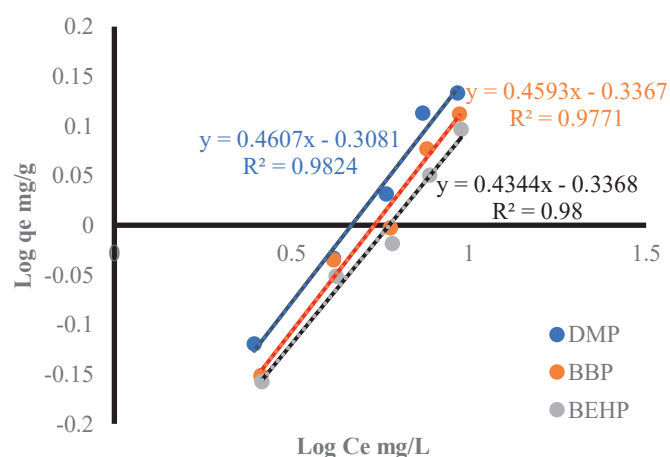
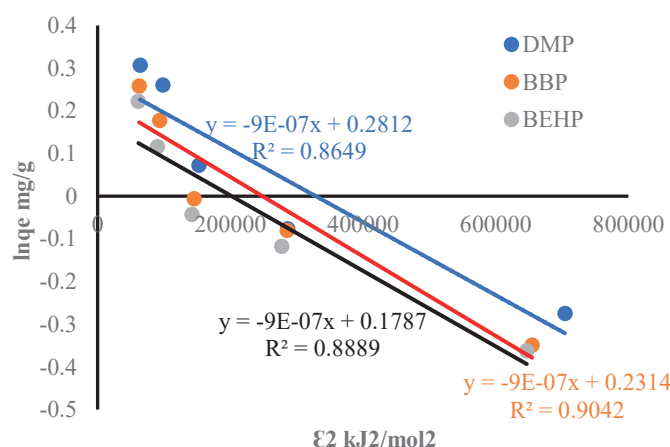
Thermodynamic Studies

The effect of temperature on phthalates adsorption onto WHB was examined in the 298–338 K temperature range. The percent removal decreased with increasing temperature, a characteristic of exothermic process. The maximum %R at 298 K was 73.03%, 72.24% and 71.46% for DMP, BBP, and BEHP, respectively (Figure 9). The fact that maximum percent removal was recorded at room temperature is significant for practical application since temperature adjustment is not required.

The decrease in %R with the temperature rise is probably due to increased solubility with an increase in temperature. The calculated thermodynamic functions are shown in Table 6.

Table 5: Adsorption Isotherm Parameters

Adsorbate	Langmuir model				Freundlich model			D-R-K model	
	Q_0	K_L	R_L	R^2	K_f	$\frac{1}{n}$	R^2	q_s	R^2
DMP	1.828	0.276	0.4753	0.9635	0.4919	0.4607	0.9824	0.911	0.8649
BBP	1.767	0.255	0.4949	0.9744	0.4606	0.4593	0.9771	1.704	0.9042
BEHP	1.618	0.286	0.4666	0.9708	0.4605	0.4344	0.980	1.509	0.8889

**Figure 5:** The percent removal of DMP, BBP, and BEHP by WHB at different concentrations**Figure 6:** Langmuir plot for DMP, BBP, and BEHP**Figure 7:** Freundlich plot for DMP, BBP, and BEHP**Figure 8:** D-R-K isotherm adsorption for DMP, BBP, and BEHP onto WHB

The negative ΔH values (Table 8) confirm that the adsorption of the phthalates onto WHB is an exothermic reaction. According to Jemutai-Kimosop et al.,³⁹ ΔH values below 40 kJ/mol denote a physisorption mechanism. In this work, all the enthalpy values were below 40 kJ/mol signifying that the adsorption of DMP, BBP, and BEHP onto WHB entails a physisorption process. This is further supported by the observations from the Freundlich and D-R-K isotherms and FTIR study. The negative ΔS values imply increased orderliness at the solid-liquid interface.

The negative ΔG values (Table 6) denote that the adsorption of the phthalates onto WHB was thermodynamically spontaneous. In general, ΔG values in the range $-20 \text{ kJ/mol} < \Delta G < 0 \text{ kJ/mol}$ imply physisorption whereas a chemisorption mechanism is implied for $-400 \text{ kJ/mol} < \Delta G < -80 \text{ kJ/mol}$.⁴⁰ The magnitudes of ΔG values (Table 6) correspond to a physical adsorption mechanism. This corroborates the earlier deductions. The thermodynamics data reveal that the adsorption of DMP, BBP, and BEHP by the WHB is an enthalpy-driven process

Effect of the Adsorbent Dosage

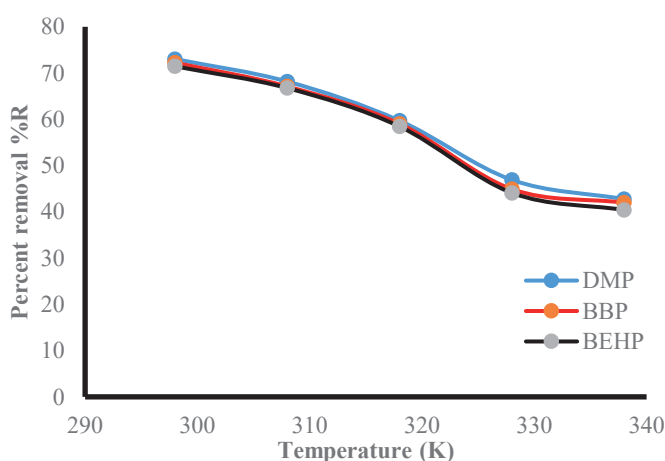
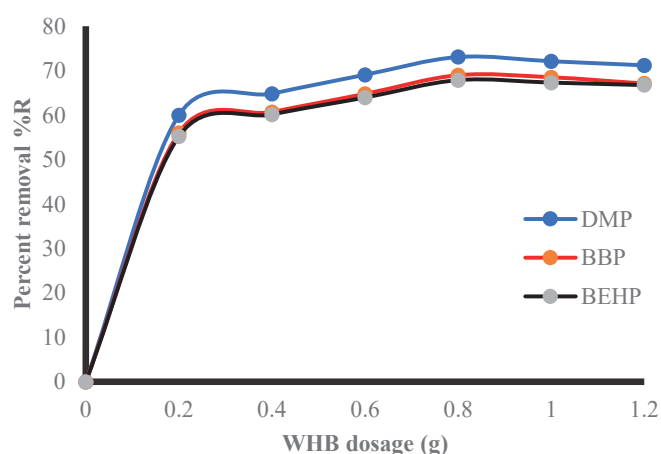
The effect of adsorbent dosage on adsorbent performance was studied in the range of 0.2g–1.2g of adsorbent in a 50 mL solution (Figure 10). The percent removal of all the phthalates increased when the adsorbent dosage increased from 0.2 to 0.8 g. This is attributed to the increase in the number of adsorption sites. The maximum %R at a WHB dosage of 0.8 g/50 mL was 73.07%, 68.97% and 67.87% for DMP, BBP and BEHP, respectively. However, beyond 0.8g/50mL dosage, there was no appreciable change in percent phthalate removal. This is due to agglomeration of the adsorption sites with an increase in the adsorbent particles.

Comparison with other adsorbents

The adsorption capacity of the water hyacinth roots derived biochar (WHB) was compared to other adsorbents reported in literature (Table 7). The differences are attributed to both precursor properties, synthesis conditions, identity of phthalate and experimental

Table 6: Thermodynamic parameters

Adsorbate	Parameter	Temperature (K)				
		298	308	318	328	338
DMP	% Removal	73.030	68.171	59.710	46.906	42.752
	ΔG (kJ/mol)	-19.583	-19.639	-19.303	-18.500	-18.591
	ΔS (J/mol)	-30.925				
	ΔH (kJ/mol)	-28.957				
BBP	% Removal	72.243	67.103	59.042	44.907	41.986
	ΔG (kJ/mol)	-19.484	-19.514	-19.230	-18.280	-18.503
	ΔS (J/mol)	-31.718				
	ΔH (kJ/mol)	-29.089				
BEHP	% Removal	71.457	66.749	58.453	44.103	40.404
	ΔG (kJ/mol)	-19.389	-19.473	-19.166	-18.191	-18.320
	ΔS (J/mol)	-33.786				
	ΔH (kJ/mol)	-29.651				

**Figure 9:** Percent phthalate removed by WHB as a function of temperature**Figure 10:** Effect of adsorbent dose on percent phthalate removal**Table 7:** Comparison with other adsorbents

Adsorbent	Phthalate	Adsorption capacity (mg/g)	Reference
Corncob biochar B700	DBP	20.23	41
Corncob biochar B900	DBP	20.26	41
Oxidized Corncob biochar AB700	DBP	22.9	41
Corncob biochar AB900	DBP	23.88	41
MWCNTs/Ag	BBP	87.72	42
UiO-67-30BA	DMP	395.3	43
Cu ₂ O-zeolite	DMP	20.41	8
WHB	BBP	1.83	This study
WHB	DMP	1.77	This study
WHB	BEHP	1.62	This study

conditions. The suitability of the adsorbents should be evaluated also based on overall cost of synthesis, scalability, environmental impact and sustainability, especially for emerging economies.

CONCLUSION

In this work, water hyacinth biochar (WHB) was used as a low-cost, eco-conscious adsorbent for the removal of three phthalates, DMP, BBP, and BEHP, from synthetic wastewater in single solute solutions. The maximum monolayer adsorption capacity was 1.83, 1.77, and 1.62 mg/g for DMP, BBP and BEHP, respectively. The

adsorption of the phthalates was inhibited by the molecular weight and kinetic diameters/bulkiness of the molecules but compensated by their hydrophobicity. The kinetic data was best predicted by the quasi-second order model (PSO) with an equilibrium time of 25 min. The equilibrium adsorption data was predicted by adsorption isotherm models in the order Freundlich>Langmuir>D-R-K. The thermodynamics functions showed that the adsorption of the phthalates onto WHB was spontaneous, exothermic, physical, enthalpically-driven, and energetically favorable. Therefore, WHB is a potential next-generation low-cost adsorbent for the removal of DMP, BBP, and BEHP from water.

STATEMENT OF COMPETING INTEREST

The authors declare no competing interest

DECLARATION OF GENERATIVE AI AND AI-ASSISTED TECHNOLOGIES

During the preparation of this work, the author(s) used Grammarly to check and proofread grammatical mistakes and punctuation. After using this tool/service, the author(s) reviewed and edited the content as needed and take(s) full responsibility for the content of the publication.

ACKNOWLEDGMENTS

We gratefully acknowledge the financial support from the National Research Fund (NRF – Kenya)

ORCID IDS

Elkanah N. Ogora: <https://orcid.org/0000-0003-3562-6372>

Zachary M. Getenga: <https://orcid.org/0000-0003-0570-7403>

Victor O. Shikuku: <https://orcid.org/0000-0002-2295-293X>

REFERENCES

- Jackson J, Sutton R. Sources of Endocrine-Disrupting Chemicals in Urban Wastewater, Oakland, CA. *Sci Total Environ.* 2008;405(1–3):153–160. <https://doi.org/10.1016/j.scitotenv.2008.06.033>.
- Iñigo-Nuñez S, Herreros MA, Encinas T, Gonzalez-Bulnes A. Estimated Daily Intake of Pesticides and Xenoestrogenic Exposure by Fruit Consumption in the Female Population from a Mediterranean Country (Spain). *Food Control.* 2010;21(4):471–477. <https://doi.org/10.1016/j.foodcont.2009.07.009>.
- Annamalai J, Namasivayam V. Endocrine Disrupting Chemicals in the Atmosphere: Their Effects on Humans and Wildlife. *Environ Int.* 2015;76:78–97. <https://doi.org/10.1016/j.envint.2014.12.006>.
- Ngeno E, Ongulu R, Orata F, Matovu H, Shikuku V, Onchiri R, Mayaka A, Majanga E, Getenga Z, Gichumbi J, et al. Endocrine Disrupting Chemicals in Wastewater Treatment Plants in Kenya, East Africa: Concentrations, Removal Efficiency, Mass Loading Rates and Ecological Impacts. *Environ Res.* 2023;237:117076. <https://doi.org/10.1016/j.envres.2023.117076>.
- Diamanti-Kandarakis E, Bourguignon J-P, Giudice LC, Hauser R, Prins GS, Soto AM, Zoeller RT, Gore AC. Endocrine-Disrupting Chemicals: An Endocrine Society Scientific Statement. *Endocr Rev.* 2009;30(4):293–342. <https://doi.org/10.1210/er.2009-0002>.
- Shikuku VO, Ngeno EC, Njewa JB, Ssebugere P. Pharmaceutical and Personal Care Products (PPCPs) and per- and Polyfluoroalkyl Substances (PFAS) in East African Water Resources: Progress, Challenges, and Future. *Basic Sci. Sustain. Dev.* 2023;2:21–38. <https://doi.org/10.1515/9783111071206-002>.
- Casajuana N, Lacorte S. Presence and Release of Phthalic Esters and Other Endocrine Disrupting Compounds in Drinking Water. *Chromatographia.* 2003;57(9–10):649–655. <https://doi.org/10.1007/BF02491744>.
- Esfandian H, Yousefi E, Sharifzadeh BM. Removal of Dimethyl Phthalate from Aqueous Solution by Synthetic Modified Nano Zeolite Using Cu₂O Nanoparticles. *Int. J. Eng. Trans. A Basics.* 2016;29(9):1198–1207. <https://doi.org/10.5829/idosi.ije.2016.29.09c.03>.
- Tapia-Orozco N, Ibarra-Cabrera R, Tecante A, Gimeno M, Parra R, Garcia-Arrazola R. Removal Strategies for Endocrine Disrupting Chemicals Using Cellulose-Based Materials as Adsorbents: A Review. *J Environ Chem Eng.* 2016;4(3):3122–3142. <https://doi.org/10.1016/j.jece.2016.06.025>.
- Fang ZQ, Huang HJ. Adsorption of Di-n-Butyl Phthalate onto Nutshell-Based Activated Carbon. Equilibrium, Kinetics and Thermodynamics. *Adsorpt Sci Technol.* 2009;27(7):685–700. <https://doi.org/10.1260/0263-6174.27.7.685>.
- Xu Z, Zhang W, Pan B, Lv L, Jiang Z. Treatment of Aqueous Diethyl Phthalate by Adsorption Using a Functional Polymer Resin. *Environ Technol.* 2011;32(2):145–153. <https://doi.org/10.1080/09593330.2010.490854>.
- Den W, Liu H-C, Chan S-F, Kin KT, Huang C. Adsorption of Phthalate Esters with Multiwalled Carbon Nanotubes and Its Application. *Adsorption* of phthalate esters with multiwalled carbon nanotubes and its applications. *J Environ Econ Manage.* 2006;16(4):275–282.
- Chen C, Chen C, Chung Y. Removal of phthalate esters by α -cyclodextrin-linked chitosan bead. *Bioresour Technol.* 2007;98(13):2578–2583. <https://doi.org/10.1016/j.biortech.2006.09.009>.
- Chan HW, Lau TC, Ang PO, Wu M, Wong PK. Biosorption of Di(2-Ethylhexyl)Phthalate by Seaweed Biomass. *J Appl Phycol.* 2004;16(4):263–274. <https://doi.org/10.1023/B:JAPH.0000047778.93467.af>.
- Ngeno EC, Mbuci KE, Necibi MC, Shikuku VO, Olisah C, Ongulu R, Matovu H, Ssebugere P, Abushaban A, Sillanpää M. Sustainable Re-Utilization of Waste Materials as Adsorbents for Water and Wastewater Treatment in Africa: Recent Studies, Research Gaps, and Way Forward for Emerging Economies. *Environ Adv.* 2022;9(August):100282. <https://doi.org/10.1016/j.envadv.2022.100282>.
- Wang H, Hua H, Zhang L, Wen S. On the Resistance-Harary Index of Graphs Given Cut Edges. *J Chem.* 2017;2017:1–7. <https://doi.org/10.1155/2017/3531746>.
- Orata F, Ngeno EC, Baraza LD, Shikuku VO, Kimosop SJ. Adsorption of Caffeine and Ciprofloxacin onto Pyrolytically Derived Water Hyacinth Biochar: Isothermal, Kinetic and Thermodynamic Studies. *J Chem Chem Eng.* 2016;10(4). <https://doi.org/10.17265/1934-7375/2016.04.006>.
- Hashem MA, Hasan M, Momen MA, Payel S, Nur-A-Tomal MS. Water Hyacinth Biochar for Trivalent Chromium Adsorption from Tannery Wastewater. *Environ. Sustain. Indic.* 2020;5:100022. <https://doi.org/10.1016/j.indic.2020.100022>.
- Liu Y, Gao Z, Ji X, Wang Y, Zhang Y, Sun H, Li W, Wang L, Duan J. Efficient Adsorption of Tebuconazole in Aqueous Solution by Calcium Modified Water Hyacinth-Based Biochar: Adsorption Kinetics, Mechanism, and Feasibility. *Molecules.* 2023;28(8):3478. <https://doi.org/10.3390/molecules28083478>.
- Bian P, Shao Q. Performance and Mechanism of Functionalized Water Hyacinth Biochar for Adsorption and Removal of Benzotriazole and Lead in Water. *Int J Mol Sci.* 2023;24(10):8936. <https://doi.org/10.3390/ijms24108936>.
- Onchiri R, Mayaka A, Majanga A, Ongulu R, Orata F, Getenga Z, Gichumbi J, Ogora E. Phthalate Levels in Wastewater Treatment Plants of Lake Victoria Basin. *Appl. Ecol. Environ. Sci.* 2025;9(12):1011–1017. <https://doi.org/10.12691/aees-9-12-4>.
- Cousins IT, Mackay D, Parkerton TF. Physical-Chemical Properties and Evaluative Fate Modelling of Phthalate Esters. Berlin Heidelberg: Springer-Verlag; 2003. pp. 57–84. <https://doi.org/10.1007/b11463>.
- Shikuku VO, Jemutai-Kimosop S. Efficient Removal of Sulfamethoxazole onto Sugarcane Bagasse-Derived Biochar: Two and Three-Parameter Isotherms, Kinetics and Thermodynamics. *S Afr J Chem.* 2020;73(1):111–119. <https://doi.org/10.17159/0379-4350/2020/v73a16>.
- Ho YS, McKay G. Sorption of Dye from Aqueous Solution by Peat. *Chem Eng J.* 1998;70(2):115–124. [https://doi.org/10.1016/S0923-0467\(98\)00076-1](https://doi.org/10.1016/S0923-0467(98)00076-1).
- Ho Y, Ofomaja A. Pseudo-second-order model for lead ion sorption from aqueous solutions onto palm kernel fiber. *J Hazard Mater.* 2006;129(1–3):137–142. <https://doi.org/10.1016/j.jhazmat.2005.08.020>.
- Weber WJ Jr, Rumer RR Jr. Intraparticle Transport of Sulfonated Alkylbenzenes in a Porous Solid: Diffusion with Nonlinear Adsorption. *Water Resour Res.* 1965;1(3):361–373. <https://doi.org/10.1029/WR001i003p00361>.
- Langmuir I. THE ADSORPTION OF GASES ON PLANE SURFACES OF GLASS, MICA AND PLATINUM. *J Am Chem Soc.* 1918;40(9):1361–1403. <https://doi.org/10.1021/ja02242a004>.
- Hall KR, Eagleton LC, Acrivos A, Vermeulen T. Pore- and Solid-Diffusion Kinetics in Fixed-Bed Adsorption under Constant-Pattern Conditions. *Ind Eng Chem Fundam.* 1966;5(2):212–223. <https://doi.org/10.1021/i160018a011>.
- Freundlich H. Über Die Adsorption in Lösungen. *Z Phys Chem.* 1907;57U(1):385–470. <https://doi.org/10.1515/zpch-1907-5723>.
- Cerofolini GF. A Model Which Allows for the Freundlich and the Dubinin-Radushkevich Adsorption Isotherms. *Surf Sci.* 1975;51(1):333–335. [https://doi.org/10.1016/0039-6028\(75\)90260-5](https://doi.org/10.1016/0039-6028(75)90260-5).
- Galhetas M, Mestre AS, Pinto ML, Gulyurtlu I, Lopes H, Carvalho AP. Carbon-Based Materials Prepared from Pine Gasification Residues for

- Acetaminophen Adsorption. *Chem Eng J.* 2014;240:344–351. <https://doi.org/10.1016/j.cej.2013.11.067>.
32. Mboka JM, Tamaguelon HD, Shikuku V, Tome S, Deugueu VF, Othman H, Janiak C, Dika MM, Etoh MA, Dina DJD. Novel Superadsorbent from Pozzolan-Charcoal Based Geopolymer Composite for the Efficient Removal of Aqueous Crystal Violet. *Water Air Soil Pollut.* 2024;235(7):430. <https://doi.org/10.1007/s11270-024-07257-4>.
33. Ngeno E, Ongulu R, Shikuku V, Ssentongo D, Otieno B, Ssebugere P, Orata F. Response Surface Methodology Directed Modeling of the Biosorption of Progesterone onto Acid Activated Moringa Oleifera Seed Biomass: parameters and Mechanisms. *Chemosphere.* 2024;360:142457. <https://doi.org/10.1016/j.chemosphere.2024.142457>.
34. Xu Y, Liu Y, Liu S, Tan X, Zeng G, Zeng W, Ding Y, Cao W, Zheng B. Enhanced Adsorption of Methylene Blue by Citric Acid Modification of Biochar Derived from Water Hyacinth (*Eichornia Crassipes*). *Environ Sci Pollut Res Int.* 2016;23(23):23606–23618. <https://doi.org/10.1007/s11356-016-7572-6>.
35. Jedynek K, Widel D, Oszczudłowski J. Removal of Selected Phthalates from Aqueous Solution by Mesoporous-Ordered Carbon Adsorbent. *Adsorpt Sci Technol.* 2017;35(7–8):744–750. <https://doi.org/10.1177/0263617417708675>.
36. Achieng G, Shikuku V. Adsorption of Copper Ions from Water onto Fish Scales Derived Biochar: isothermal Perspectives. *J Mater Environ Sci.* 2020;2020(11):1816–1827.
37. Krupadam RJ, Sridevi P, Sakunthala S. Removal of Endocrine Disrupting Chemicals from Contaminated Industrial Groundwater Using Chitin as a Biosorbent. *J Chem Technol Biotechnol.* 2011;86(3):367–374. <https://doi.org/10.1002/jctb.2525>.
38. Dada AO, Olalekan AP, Olatunya AM, Dada O. Langmuir, Freundlich, Temkin and Dubinin–Radushkevich Isotherms Studies of Equilibrium Sorption of Zn^{2+} Unto Phosphoric Acid Modified Rice Husk. *IOSR J Appl Chem.* 2012;3(1):38–45. <https://doi.org/10.9790/5736-0313845>.
39. Jemutai-Kimosop S, Okello VA, Shikuku VO, Orata F, Getenga ZM. Synthesis of Mesoporous Akaganeite Functionalized Maize Cob Biochar for Adsorptive Abatement of Carbamazepine: Kinetics, Isotherms, and Thermodynamics. *Clean Mater.* 2022;5(June):100104. <https://doi.org/10.1016/j.clema.2022.100104>.
40. Dzoujo HT, Shikuku VO, Tome S, Akiri S, Kengne NM, Abdpour S, Janiak C, Etoh MA, Dina D. Synthesis of Pozzolan and Sugarcane Bagasse Derived Geopolymer-Biochar Composites for Methylene Blue Sequestration from Aqueous Medium. *J Environ Manage.* 2022;318(March):115533. <https://doi.org/10.1016/j.jenvman.2022.115533>.
41. Abdoul ASI, Islam MS, Chen Y, Weng L, Sun Y, Chang X, Zhou B, Ma J, Li Y. Competitive adsorption of Dibutyl phthalate (DBP) and Di(2-ethylhexyl) phthalate (DEHP) onto fresh and oxidized corncob biochar. *Chemosphere.* 2021;280:130639. <https://doi.org/10.1016/j.chemosphere.2021.130639>.
42. Falahrodbari S. Adsorption of Benzene Butyl Phthalate with Mullti-walled Carbon Nanotubes/Ag nanoparticles and its Applications. *Orient J Chem* 2017;33(2):330241. <http://dx.doi.org/10.13005/ojc/330241>.
43. Liu Q, Ye J, Han Y, Wang P, Fei Z, Chen X, Zhang Z, Tang J, Cui M, Qiao X. Defective UiO-67 for enhanced adsorption of dimethyl phthalate and phthalic acid. *J. Mol. Liq.* 2020;321:114477. <https://doi.org/10.1016/j.molliq.2020.114477>.